Current Science
CS 5 (3), 3193-3207 (2025)
Received 19 March 2025 | **Revised 22 April** 2025 | **Accepted 26 May**. 2025 | **Online Available 20 June** 2025
https://doi.org/ 10.52845/CS/2025-5-3-86

Current Science

Current Science

OPEN ACCESS

ISSN(O)2795-8639

Original Article

Allyl Methyl Sulfone Attenuates Oxidative Stress and Inflammation in Fibroblast-Like Synoviocytes via NF-Kb P65/SLC7A11 Signaling iin Osteoarthritis

Zihao Dong[1*], Yong Zhang[2*], Bin Li[2], Cuiling Gao[3], Guodong Wang[4], Guang Yang[1,3]

[1]Department of Joint Surgery, Shandong Provincial Hospital Affiliated to Shandong First Medical University, Jinan 250021, Shandong, P. R. China

[2]Shandong Institute for Product Quality Inspection, Jinan 250014, Shandong, P. R. China

[3]Metabolism and Disease Research Center, Central Hospital Affiliated to Shandong First Medical University, Jinan 250013, Shandong, P.R. China

[4]Department of Orthopedics, Zouping Traditional Chinese Medicine Hospital, Zouping 256200, Shandong, P. R. China

***These Authors Contributed Equally to this Work.**

[*]Corresponding Author: Guang Yang

Abstract:
Allyl methyl sulfone ($AMSO_2$) is an oxidative metabolite derived from allyl methyl sulfide, a major garlic component. $AMSO_2$ has been demonstrated to exert anti-inflammatory and antioxidative effects; however, its effect on arthritis has not yet been thoroughly studied. Overactivation and uncontrolled proliferation of synoviocytes are the major causes of arthritis progression, which is characterized by persistent inflammation. In the present study, we found that $AMSO_2$ could alleviate the osteoarthritis (OA) progression in mice models, and inhibit inflammatory response in tumor necrosis factor α (TNFα)-stimulated human fibroblast-like synoviocytes (FLSs) by suppressing the expression of cytokines and chemokines, such as C–C motif chemokine ligand 2 (CCL2), interleukin (IL)-6, interleukin (IL)-8. $AMSO_2$ also reduced oxidative stress by downregulating the expression of inducible nitric oxide synthase (iNOS) and inhibiting the production of reactive oxygen species (ROS). Furthermore, the expression and secretion of matrix metalloproteinases were significantly reduced by $AMSO_2$. This study also showed that the effect of $AMSO_2$ on FLSs was exerted through the nuclear factor kappa-B (NF-κB) signaling pathways, with SLC7A11 and glutathione peroxidase 4 (GPX4) being the downstream factors. Overall, these findings indicate that $AMSO_2$ regulates synovial inflammation in arthritis, thereby serving as a potential target for arthritis treatment.

Keywords: Arthritis; Fibroblast-like synoviocytes; Inflammation; NF-κB; AMSO2

1. Introduction

Arthritis is a degenerative joint disease that causes stiffness, pain, and even activity limitation in patients; it affects more than 240 million people worldwide (Katz, Arant, & Loeser, 2021). The progression of arthritis is characterized by synovial inflammation, cartilage damage, and subchondral bone thickening. Under normal conditions, fibroblast-like synoviocytes (FLSs) constitute the intimal layer of the synovial membrane and function to ensure smooth joint articulation (Mathiessen & Conaghan, 2017). In recent years, the contributions of FLSs to arthritis development have gained increasing attention, such as in rheumatoid arthritis (RA) and

osteoarthritis (OA). In chronic inflammation, FLSs become dysregulated and hyperproliferative and transform into an aggressive phenotype, thereby promoting joint destruction (Perez-Garcia et al., 2019). In addition, the accumulation of FLSs in the intima leads to synovial hyperplasia and secretion of cartilage-degrading enzymes, such as matrix metalloproteinases (MMPs) (Qin et al., 2022). Therefore, FLSs can be considered a target for arthritis treatment. However, the pathogenic role of synovial tissue inflammation in early and advanced arthritis remains unclear.

Inflammatory cytokines are critical mediators in the pathological process of OA (Mathiessen & Conaghan, 2017). Notably, tumor necrosis factor α (TNFα) stimulates FLS activation (Mathiessen & Conaghan, 2017; (Xie & Chen, 2019) and releases interleukin (IL)-6, IL-1β, cyclooxygenase 2 (COX-2), and prostaglandin E2 (PGE2) (S. Liu et al., 2019). A recent study demonstrated that C–C motif chemokine ligand 2 (CCL2) was elevated in patients with OA, thereby contributing to monocyte and macrophage recruitment (Haraden, Huebner, Hsueh, Li, & Kraus, 2019). Furthermore, knockout of C–C motif chemokine receptor 2 (CCR2) alleviated OA-induced inflammation and pain in mouse models (Raghu et al., 2017). The secreted cytokines have been reported to promote monocyte recruitment, which further aggravates tissue inflammation injury and leads to arthritis progression (Chen et al., 2019).

The nuclear factor kappa-B (NF-κB) signaling pathway is one of the most important regulators of inflammation. Persistent NF-κB activation has been demonstrated to increase the expression of TNFα, IL-6, IL-8, CCL2, and MMPs, thereby promoting OA progression (Bao et al., 2020). In addition, the NF-κB signaling pathway promotes cystine uptake and cellular (glutathione) GSH production, thereby protecting synovial fibroblasts from lipid peroxidation and ferroptosis (S. Li et al., 2021). Thus, inhibiting NF-κB pathway activation is an attractive treatment approach for arthritis.

Our previous studies have demonstrated that organosulfide compounds exert anti-inflammatory and oxidative effects (G. Yang et al., 2020). Allyl methyl sulfone ($AMSO_2$) is a major metabolite of aged garlic extract *in vivo* (Y. Liu et al., 2019). Major components of garlic, such as allyl methyl sulfide (AMS), S-allyl-L-cysteine, and S-allylmercaptocysteine (SAMC), were quickly metabolized in rat erythrocytes through the mechanisms of reduction, methylation, and oxidation (Y. Liu et al., 2019; (M. Yang et al., 2018). Studying the properties of these metabolites is necessary for further drug development and therapeutic target discovery. Previous research has demonstrated that $AMSO_2$ exerts anti-inflammatory and anti-oxidative effects as well as antiapoptotic effect in lung injuries in rats via the ERK/p38 MAPK and NF-κB signaling pathways (A. Li et al., 2018). However, the pharmacological effect of $AMSO_2$ in arthritis and its underlying mechanism need to be elucidated further.

In this study, we conducted both *in vivo* and *in vitro* experiments to assess the role of $AMSO_2$ in OA model, and using human FLSs stimulated with TNFα to mimic the inflammatory microenvironment of arthritis. Our findings indicated that $AMSO_2$ exerted modulatory effects on inflammation, oxidative stress, and cartilage degradation in TNFα-treated FLSs. Verification of the mechanism of $AMSO_2$ can facilitate the development of therapeutic approaches for patients with arthritis.

1. Materials and Methods

2.1 Reagents

$AMSO_2$ (718203) (Fig. 1A), with a purity of 96%, and TNFα (T6674) were obtained from Sigma-Aldrich (USA). PS-1145 (GC17603) was purchased from GlpBio (USA). Rabbit anti-SLC7A11 (26864-1-AP) and rabbit anti-β-actin (20536-1-AP) were purchased from Proteintech (USA). Rabbit anti-GPX4 (ab125066) was purchased from Abcam (USA). Rabbit anti-Lamin B1 (D4Q4Z) (#12586), rabbit anti-NF-κB p65 (C22B4) (#4764), and rabbit anti-IκBα (#9242) antibodies were purchased from Cell Signaling Technology (USA).

2.2 Cell Culture and Treatment

Human monocytic cell line (THP-1) was obtained from the cell bank of Chinese Academy of Sciences (Shanghai, China). THP-1 cells were cultured in RPMI 1640 medium (BI, Israel) supplemented with 10% fetal bovine serum (FBS, Gibco, USA) and 1% penicillin/streptomycin (Solarbio, China) at 37°C and 5% CO_2.

FLSs were isolated and cultured as previously

described (Dasuri et al., 2004) from the synovial tissue collected from 10 patients undergoing hip or knee replacement. The age of the patients with OA was between 51 and 67 years, and 4 and 6 of them were men and women, respectively (Table S1).

Table S1. Characteristics of OA individuals for isolation of synovial fibroblasts.

Sex	Age	Disease	Surgery
Female	60	hip OA	THR
Male	57	knee OA	TKA
Female	62	knee OA	TKA
Female	70	knee OA	TKA
Female	62	knee OA	TKA
Male	57	hip OA	THR
Female	51	hip OA	THR
Male	65	knee OA	TKA
Male	66	knee OA	TKA
Female	66	knee OA	TKA

*** OA: osteoarthritis; THR: total hip replacement; TKA: total knee replacement.**

The collected tissues were diced and digested in 0.15% trypsin at 37°C for 2 h. The trypsinized samples were then incubated in 3 mg/mL collagenase type I at 37°C overnight. Subsequently, the cells were centrifuged and suspended in Dulbecco's Modified Eagle Medium/Ham's F-12 (DMEM/Ham's 12, BI, Israel) supplemented with 10% FBS, 2 mM L-glutamine (Gibco, USA), and 1% penicillin/streptomycin overnight. The nonadherent cells were discarded, and the adherent cells were cultured in fresh medium at 37°C in 5% CO_2 until the cell layers were confluent. All experiments were conducted in accordance with the ethical principles of the World Medical Association Declaration of Helsinki for Medical Research Involving Human Subjects, and written informed consent was obtained from all participants. The study protocol was approved by the ethics committee of Shandong Provincial Hospital (NO. 2022-819).

2.3 Cell Viability Assay

Cell viability was assessed via CCK8 assay. In brief, cells (2×10^3/well) were plated in 96-well plates and treated with 10 ng/mL TNFα in the presence or absence of $AMSO_2$ for 24 h. Then, 10 μL of WST-8 solution was added to the treated cells and incubated at 37°C and 5% CO_2 for additional 4 h. Cell viability was detected by measuring absorbance at 450 nm using a microplate reader (BioTek Synergy 2, USA).

2.4 Monocyte Adhesion Assay

Monocyte adhesion to FLSs was evaluated using fluorescence-labeled THP-1 cells as previously described (Ishii et al., 2018). In brief, FLSs were seeded in 24-well plates overnight and treated with TNFα (10 ng/mL) in serum-free DMEM for 16 h. The THP-1 cells were labeled with CellTracker CMFDA (C2925, Invitrogen) and cocultured with FLSs for 15 min at 37°C. Then, each well was washed three times with phosphate-buffered saline (PBS) to separate nonadherent monocytes. The adherent cells were quantified by measuring fluorescence at an excitation of 485/20 nm and emission of 528/20 nm using a fluorescence plate reader (Bio Tek Synergy 2, USA).

2.5 Real-time Polymerase Chain Reaction

Total RNA was extracted from FLSs using QIAzol reagent (Qiagen, Germany) in accordance with the manufacturer's instructions. NanoDrop spectrophotometry was used to determine the quantity and quality of the extracted RNA. For RT-PCR, 2 μg of total RNA was reverse-transcribed to produce cDNA using an iScript RT-PCR Kit from Bio-Rad (USA). The synthesized cDNA was used to detect the mRNA expression of the target genes via real-time PCR on an ABI 7500 Real-Time PCR platform (Applied Biosystems, USA) using the SYBR Green method. Glyceraldehyde-3-phosphate dehydrogenase was used as the internal

housekeeping gene. The relative expression levels of the target genes were calculated using the $2^{-\Delta\Delta Ct}$ method. Table 1 presents the primer sequences of targeted genes.

Table 1. The primer sequences of targeted genes for real-time PCR.

Homo sapiens	Forward	Reverse
MMP-1	5′-GCCAGATTTGCCAAGAGCAG-3′	5′-GCTTGACCCTCAGAGACCTT-3′
MMP-3	5′-GATGCCCACTTTGATGATGATGAA-3′	5′-AGTGTTGGCTGAGTGAAAGAGACC-3′
MMP-13	5′-TCTTCGGCTTAGAGGTGACTG-3′	5′-CAGAGGAGTTACATCGGACCA-3′
IL-6	5′-GAAAGCAAAGAGGCACT-3′	5′-TTTCACCAGGCAAGTCTCCT-3′
IL-8	5′-GGCTTGCTAGGGGAAATGA-3′	5′-AGCTGACTCTGACTAGGAAACTT-3′
CCL2	5′-CAGCCACCTTCATTCCCCAA-3′	5′-GGACACTTGCTGCTGGTGAT-3′
CCL5	5′-TCATTGCTACTGCCCTCTGC-3′	5′-TCGGGTGACAAAGACGACTG-3′
GAPDH	5′-CACATGGCCTCCAAGGAGTAA-3′	5′-TGAGGGTCTCTCTCTTCCTCTTGT-3′

2.6 Western Blot Analysis

Proteins from cells were lysed using RIPA lysis and extraction buffer (25 mM Tris–HCl [pH 7.6], 150 mM NaCl, 1% NP-40, 1% sodium deoxycholate, 0.1% SDS) or NE-PER™ Nuclear and Cytoplasmic Extraction Reagents (78833, Thermo Scientific, USA), with the protease and phosphatase inhibitor cocktail (ab201119, Abcam, USA). Subsequently, the cells were centrifuged at 15,000 × rpm at 4°C for 15 min, and the supernatant was collected for analysis. Then, 20 μg protein was separated according to size via SDS-PAGE and transferred onto PVDF membranes. Then, the membranes were blocked with 5% non-fat milk in 10 mM Tris–HCl containing 150 mM NaCl and 0.5% Tween 20 (TBS-T) for 1 h. Next, the membranes were washed with TBS-T three times and incubated with primary antibodies (1:1,000) overnight at 4°C, followed by thorough washing with TBS-T and incubation with horseradish peroxidase-conjugated secondary antibodies for 1 h. Blots were developed using an enhanced chemiluminescence detection kit (Amersham, USA).

2.7 Enzyme-linked Immunosorbent Assay (ELISA)

Specific ELISA kits, including Human MMP-1 ELISA Kit (Cat#SEKH-0251, Solarbio, Beijing), Human MMP-3 ELISA Kit (Cat# SEKH-0254, Solarbio, Beijing), and Human MMP-13 ELISA Kit (Cat#SEKH-0259, Solarbio), were used to determine the protein secretion of the target genes. In brief, 2×10^5 cells/cm^2 were seeded into 6-well plates and incubated for 24 h. Then, the supernatants were collected and subjected to ELISA analysis using the kits in accordance with the manufacturer's instructions. The results were calculated using a standard curve.

2.8 Determination of Reactive Oxygen Species (ROS) Production

The production of ROS was determined using the probe dichlorodihydrofluorescein diacetate (DCFH-DA) (S0033M, Beyotime). After the indicated treatment, the cells were washed with PBS and incubated with 10 μM DCFH-DA at 37°C for 30 min in the dark. Subsequently, the cells were imaged using a fluorescence microscope (Nikon). The fluorescence intensity of the stained cells was quantified using the Image J software (NIH, USA).

2.9 Animal Model

The study involved 20 male C57BL/6 mice, aged 8 weeks, sourced from the Beijing Vital River Laboratory Animal Technology Co., Ltd. The animals were housed under standard conditions, with a 12-hour light-dark cycle and access to food and water ad libitum. Unilateral knee osteoarthritis was induced using the destabilization of the medial meniscus (DMM)

procedure, as previously described. During the surgical procedure, mice were anesthetized with isoflurane and oxygen under sterile conditions. A small incision (3–5 mm) was made in the medial para-patellar region of the right hind limb. The joint capsule adjacent to the patellar tendon was then carefully incised to expose the medial meniscotibial ligament (MMTL). The MMTL was subsequently transected to induce DMM.

Mice were randomly divided into 5 treatment groups. Each group underwent consecutive intra-articular injections, with the initial injection administered 7 days post-DMM surgery. $AMSO_2$ were dissolved in sterile saline containing 20% HP-β-CD (Hydroxypropyl β Cyclodextrin), and the experimental group received $AMSO_2$ (100 mg/kg) (Jiang et al., 2024) with intra-articular injection three times per week for the subsequent five consecutive weeks. At the end of treatment, animals were euthanized, and knee joints were collected for histological analysis.

Animal experiments were conducted following the guidelines of the National Research Council's Manual for the Treatment and Utilization of Laboratory Animals. All the experiments were also approved by the Animal Care and Use Committee of Shandong Provincial Hospital (NO. 2022-819).

2.10 Pathological Examination

The knees were initially fixed in a 4% paraformaldehyde fix solution for 72 hours. Subsequently, they were decalcified using an EDTA solution (EDT-X, Solarbio) over a period of 28 days, after which they were embedded in paraffin wax. For the assessment of cartilage damage, frontal sections with a thickness of 6 μm were prepared. These sections were stained with hematoxylin and eosin (H&E), Safranin O and Fast Green (SF) dyes, and Toluidine Blue O (TB). Cartilage degeneration was evaluated by three blinded observers based on the guidelines provided by the Osteoarthritis Research Society International (OARSI).

2.9 Data Collection

All microarray data were downloaded from the Gene Expression Omnibus (GEO) database (http://www.ncbi.nih.gov/geo). Raw data were downloaded as MINiML files. Box plots are drawn by boxplot. The R software package "ggord" was used to draw PCA plot.

2.10 Statistical Analysis

Data from all experiments are presented as mean ± standard deviation (SD). Statistical analysis was conducted using SPSS version 21.0. For all experimental results, one-way analysis of variance (ANOVA) followed by Bonferroni's *post hoc* test was used to assess differences between the groups. P values <0.05 were considered statistically significant.

2. Results

3.1 $AMSO_2$ Inhibited the Expression of MMPs in FLSs

To select the appropriate dose of $AMSO_2$, a wide range of doses (10, 50, 100, 200, 500, 800, and 1,000 μM) was used in the CCK8 assay. $AMSO_2$ exhibited low toxicity to FLSs even at the highest dose (1,000 μM) (Fig. 1B).

Overproliferation of FLSs induces extracellular matrix (ECM) synthesis and synovial hypertrophy, which causes chronic pain and stiffness, a symptom of late-stage arthritis. MMPs are well recognized as the main substances involved in collagen cleavage and cartilage destruction. ROS overproduction is closely associated with cartilage damage (Bolduc, Collins, & Loeser, 2019). TNFα and oxidative stress promote MMP production in inflammatory FLSs; MMP-1, MMP-3, and MMP-13 have been demonstrated to play significant roles in arthritis development. Therefore, we determined the effect of $AMSO_2$ on the TNFα-induced expression of MMPs. In FLSs treated with TNFα alone, the mRNA expression of MMP-1, MMP-3, and MMP-13 increased by 3.5-, 3.8-, and 4.1-folds, respectively, whereas $AMSO_2$ dose-dependently reduced the expression of these three enzymes by roughly 2-fold (Fig. 1C). Similar results were obtained for the protein expression of MMP-1, MMP-3, and MMP-13 (Fig. 1D). Thus, $AMSO_2$ may inhibit cartilage degradation by downregulating MMP production in inflammatory FLSs.

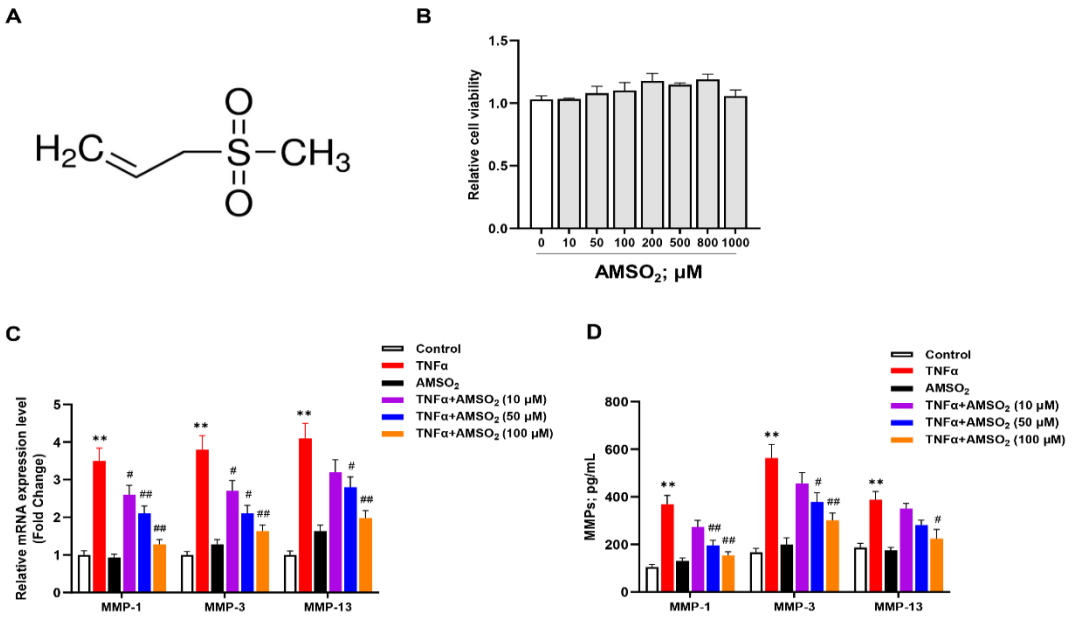

Figure 1. Effects of $AMSO_2$ on TNFα-induced matrix metalloproteinase (MMP) changes in fibroblast-like synoviocytes (FLSs). (A) Molecular structure of allyl methyl sulfone ($AMSO_2$). (B) Cell viability was measured via CCK8 assay of $AMSO_2$-treated FLSs. FLSs were stimulated with TNFα (10 ng/mL) in the presence or absence of $AMSO_2$ for 24 h. (C) mRNA levels of MMP-1, MMP-3, and MMP-13. (D) The protein expression of MMP-1, MMP-3, and MMP-13 was measured by ELISA. All experiments were conducted in triplicate. *, $P < 0.05$ vs. control group; **, $P < 0.01$ vs. control group; #, $P < 0.05$ vs. TNFα group; ##, $P < 0.01$ vs. TNFα group.

3.2 $AMSO_2$ reduced ROS Production and Oxidative Stress in FLSs

Oxidative stress is often involved in the pathophysiological process of OA and promotes synovial inflammation, chondrocyte apoptosis, and ECM degradation (Cai et al., 2021). ROS overproduction in FLSs leads to oxidative stress and is closely associated with cartilage damage (Bolduc et al., 2019). ROS production was determined using the dye DCFH-DA. After treatment of FLSs for 24 h, ROS production was increased by TNFα alone by roughly 3.5-fold and decreased by $AMSO_2$ by 2.6-, 1.9-, and 1.3-folds at concentrations of 10, 50, and 100 μM, respectively (Fig. 2A). These results suggest that $AMSO_2$ regulates the oxidant/antioxidant imbalance of OA–FLS.

In OA synovium, iNOS induces local overproduction of NO, thereby promoting inflammation, angiogenesis, and joint damage (Ostojic, Zevrnja, Vukojevic, & Soljic, 2021). Next, we measured the expression of iNOS in FLSs exposed to TNFα in the presence or absence of $AMSO_2$. TNFα was found to increase iNOS expression by nearly 2-fold. In cells treated with $AMSO_2$, iNOS expression was further increased in FLSs (Fig. 2B).

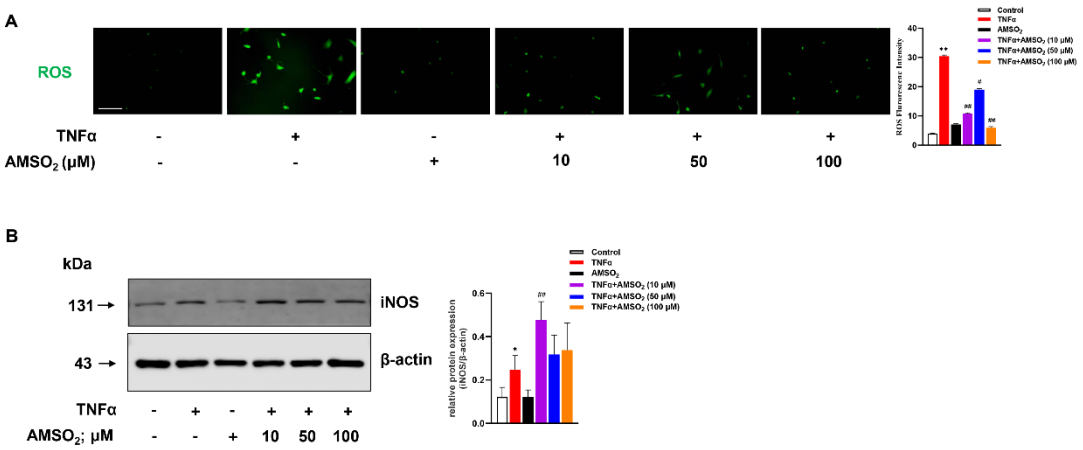

Figure 2. Effects of $AMSO_2$ on TNFα-induced oxidative stress in FLSs. FLSs were stimulated with TNFα (10 ng/mL) in the presence or absence of $AMSO_2$ (10, 50, and 100 μM) for 24 h. (A) The production of reactive oxygen species (ROS) was measured using DCFH-DA probe. Scale bar: 100 μm. (B) iNOS expression was examined via western blotting. All experiments were conducted in triplicate. *, *P* < 0.05 vs. control group; **, *P* < 0.01 vs. control group; #, *P* < 0.05 vs. TNFα group; ##, *P* < 0. 01 vs. TNFα group.

3.3 $AMSO_2$ Reduced the Expression of Inflammatory Cytokines and Chemokines and Induced Monocyte Adhesion to FLSs

ROS production has been suggested to contribute to proinflammatory and immune responses. Previous research revealed that inhibition of the expression of cytokines and chemokines produced by synoviocytes alleviated the symptoms of patients with RA (Nygaard & Firestein, 2020). In TNFα-induced FLSs, the mRNA levels of proinflammatory cytokines IL-6 and IL-8 increased by 4.3- and 3.6-folds, respectively (Fig. 3A). However, $AMSO_2$ dose-dependently reduced their expression. On the other hand, the mRNA levels of chemokines CCL2 and CCL5 increased by 7.1- and 3.1-folds, respectively (Fig. 3B). Nevertheless, $AMSO_2$ reduced the production of chemokines, particularly CCL2. Thus, $AMSO_2$ is suggested to alleviate inflammation by inhibiting proinflammatory cytokines and chemokines.

Activated FLSs are the main cause of inflammatory cytokine release, which consequently influences immune response (Mateen, Zafar, Moin, Khan, & Zubair, 2016). Cytokines and chemokines, particularly CCL2, intercellular adhesion molecule (ICAM), and vascular cell adhesion molecule (VCAM), attract monocytes to the joint cavity of patients with OA (Chen et al., 2020). To explore the immune response of $AMSO_2$ in the regulation of TNFα-induced FLS inflammation, monocyte adhesion assay was conducted. In this study, THP-1 cells were used as a model to examine monocyte adhesion to FLSs. Consistent with the anti-inflammatory effect of $AMSO_2$ in TNFα-induced FLSs, $AMSO_2$ reduced the adhesion of THP-1 cells to FLSs (Fig. 3C).

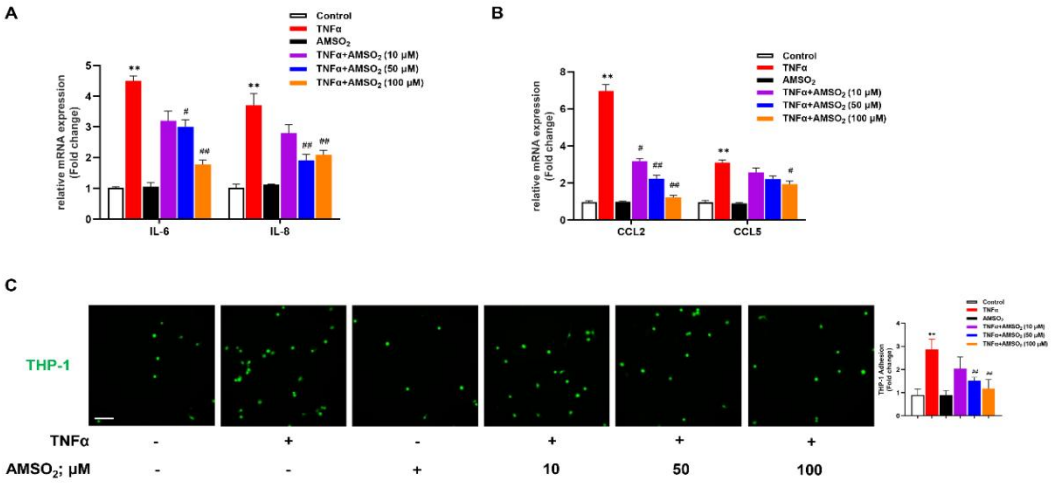

Figure 3. Effects of $AMSO_2$ on TNFα-induced expression of cytokines and monocyte adhesion in FLSs. FLSs were stimulated with TNFα (10 ng/mL) in the presence or absence of $AMSO_2$ (10, 50, and 100 μM) for 24 h. (A) mRNA level of IL-6 and IL-8; (B) mRNA level of CCL2 and CCL5. (C) FLSs were then incubated with CMFDA-labeled human THP-1 cells for 30 min. Adhesion of THP-1 cells was observed under a microscope (scale bar: 50 μm) and assessed using a fluorescence plate reader. All experiments were conducted in triplicate. *, $P < 0.05$ vs. control group; **, $P < 0.01$ vs. control group; #, $P < 0.05$ vs. TNFα group; ##, $P < 0.01$ vs. TNFα group.

3.4 $AMSO_2$ Activated the NF-κB Signaling Pathway in FLSs

$AMSO_2$ is the metabolite of SAMC *in vivo*. As previously reported, SAMC regulates the Nrf2/NF-κB pathway in OA (G. Yang et al., 2020). The NF-κB proinflammatory pathway is a major regulator of inflammation in OA and other inflammatory diseases. Exposure of FLSs to TNFα increased the nuclear level of NF-κB p65 while downregulating IκB, indicating the activation of the NF-κB signaling pathway; however, $AMSO_2$ reversed this effect (Fig. 4A).

To verify the mechanism of $AMSO_2$, PS1145 was used to inhibit IKK-mediated IκB phosphorylation. In TNFα-treated FLSs, $AMSO_2$-triggered NF-κB activation was inhibited by PS1145 (Fig. 4B). Thus, the effects of $AMSO_2$ may be mediated by regulating the NF-κB pathway in FLSs.

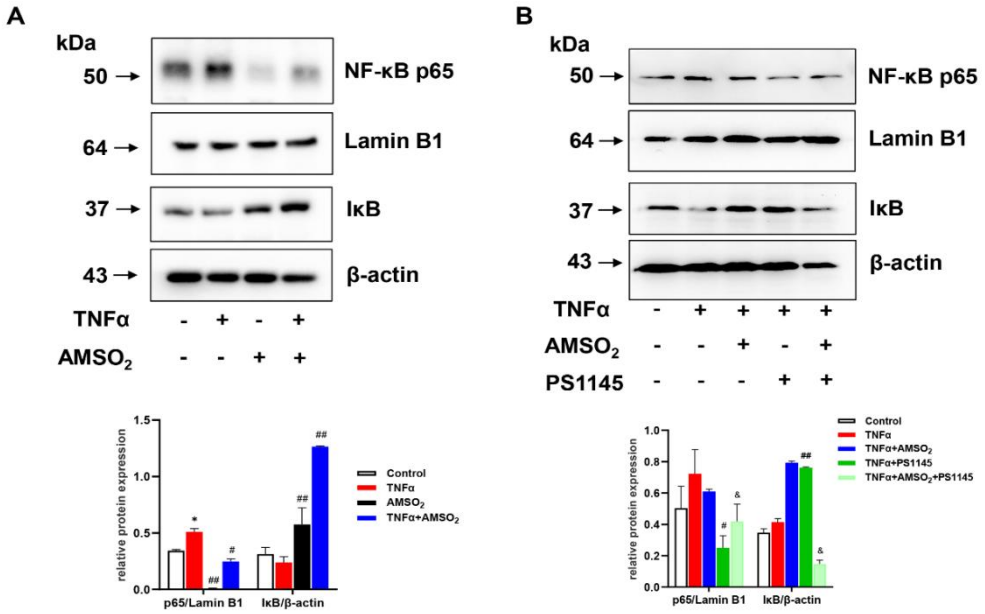

Figure 4. Effects of $AMSO_2$ on the regulation of the NF-κB pathway of TNFα-induced FLSs. (A) FLSs

were stimulated with TNFα (10 ng/mL) in the presence or absence of $AMSO_2$ (50 μM) for 6 h. The nuclear levels of NF-κB p65 and cytosolic levels of IκB were tested via western blotting; lamin B1 and β-actin were used as internal controls. (B) The IκB kinase (IKK) inhibitor PS1145 was used in $AMSO_2$-treated FLSs to test the protein expression of NF-κB p65 and IκB. Data were expressed as mean ± SD. All experiments were conducted in triplicate. *, *P* < 0.05 vs. control group; **, *P* < 0.01 vs. control group; #, *P* < 0.05 vs. TNFα group; ##, *P* < 0. 01 vs. TNFα group; &, *P* < 0.05 vs. TNFα+$AMSO_2$ group.

3.5 SLC7A11 is the Downstream Target of $AMSO_2$-treated FLSs

To investigate the association between NF-κB and ferroptosis in OA synovium, human synovia from healthy individuals and those with OA were analyzed from the data of the GEO dataset GSE1919; ferroptosis-related genes (Table S2) are presented in a heatmap (Fig. 5A–B). Antiferroptosis genes (*Gpx4* and *Slc7a11*) were found to be elevated in the synovial tissues of patients with OA compared with those of healthy individuals (Fig. 5C). SLC7A11 is a component of the Xc-transporter for cysteine/glutamine and regulates the GPX4 axis to balance the lipid ROS levels, thereby contributing to ferroptosis. The expression of SLC7A11 and GPX4 was examined in $AMSO_2$-treated FLSs. Similar to the changes of NF-κB, $AMSO_2$ decreased the expression of SLC7A11 and GPX4 in inflammatory FLSs (Fig. 5D). However, inhibition NF-κB activity by PS1145, enhanced AMSO2-triggered ferroptosis (Fig. 5E), indicating the effects of $AMSO_2$ mediated ferroptosis of inflammatory FLSs through the NF-κB pathway.

Table S2. The ferroptosis-related genes in human synovium from healthy and OA patients from GEO data sets GSE1919.

Groups	**NA**	**Normal**	**Normal**	**Normal**	**Normal**	**Normal**	**OA**	**OA**	**OA**	**OA**	**OA**
	Pvalue	GSM34379	GSM34383	GSM34385	GSM34388	GSM34391	GSM34393	GSM34394	GSM34395	GSM34396	GSM34397
acsl4	0.15079	3.42199	3.67225	3.48967	3.92699	4.55327	7.49776	7.56428	3.5386	5.79033	3.73304
alox15	0.05556	2.895	3.09279	2.17104	2.92392	4.75738	3.74945	4.94746	3.46426	3.93098	5.60585
atp5mc3	0.00794	8.68977	8.67633	8.5536	8.00272	8.47478	72.2097	70.5887	106.218	72.2203	83.1298
cars	0.00794	7.4295	7.77803	7.90776	7.62636	8.19278	43.8377	46.9101	43.6784	38.3246	35.1837
cdkn1a	0.00794	10.3787	10.1075	10.4723	9.43999	10.5949	135.994	77.9742	65.048	136.788	115.2
cs	0.00794	8.76391	8.97129	9.08134	8.48013	9.13268	95.4949	97.458	74.9332	94.5896	77.2848
dpp4	1	4.31074	3.97262	3.22454	3.81668	2.70174	4.42829	2.79695	2.60632	3.42421	5.02956
emc2	0.00794	3.97262	4.7765	5.66421	5.01651	3.74073	13.8069	9.76321	10.6045	10.9198	13.8087
fdft1	0.00794	6.30836	5.69218	6.13739	5.69789	6.12949	17.5941	14.4325	16.0592	14.1815	12.2498
gls2	1	2.17104	2.01897	1.39776	1.39776	4.13222	1.05316	3.69201	1.91512	3.05596	1.71014
gpx4	0.00794	10.0957	10.4723	10.1004	9.49335	9.68828	246.666	203.362	219.929	264.259	235.008
hspa5	0.00794	9.5482	9.7034	9.25871	9.75413	9.29489	108.193	112.439	100.448	110.643	90.756
hspb1	0.01167	11.3282	11.2776	11.2932	11.3159	11.2776	472.862	423.206	379.411	508.612	472.862
lpcat	0.00	6.3738	6.9832	6.3050	6.4635	7.2082	16.756	23.951	18.135	22.733	22.647

3	794	9	5	9		9	8	2	6	6	
mt1g	0.00794	6.86109	7.15455	6.98334	7.60138	8.322	17.3265	19.1303	41.2546	39.8844	55.7929
ncoa4	0.00794	7.56272	8.34468	9.21416	8.88581	7.31393	138.795	122.989	81.3464	62.5062	113.327
nfe2l2	0.00794	7.49881	7.51572	7.8679	7.36469	4.91867	66.3479	42.9158	45.4288	37.913	45.1412
rpl8	0.00794	12.0075	11.8589	11.773	11.7431	11.8462	836.63	815.073	844.196	797.926	736.537
sat1	0.00794	7.84907	7.53185	7.4295	7.1118	7.0002	37.6177	33.7615	154.274	29.6767	36.9288
slc1a5	0.00794	8.5861 3	8.2946 2	8.6231 7	8.1760 6	8.9131 6	49.213 5	54.469 1	48.961 3	90.531 9	43.372 4
slc7a11	0.00794	4.99059	5.99125	5.40862	5.89538	5.42756	12.0898	19.0261	11.1091	14.3927	15.9532
tfrc	0.00794	5.02981	4.59328	4.01519	3.76713	3.67352	7.73576	7.45782	9.16822	8.24847	11.1343

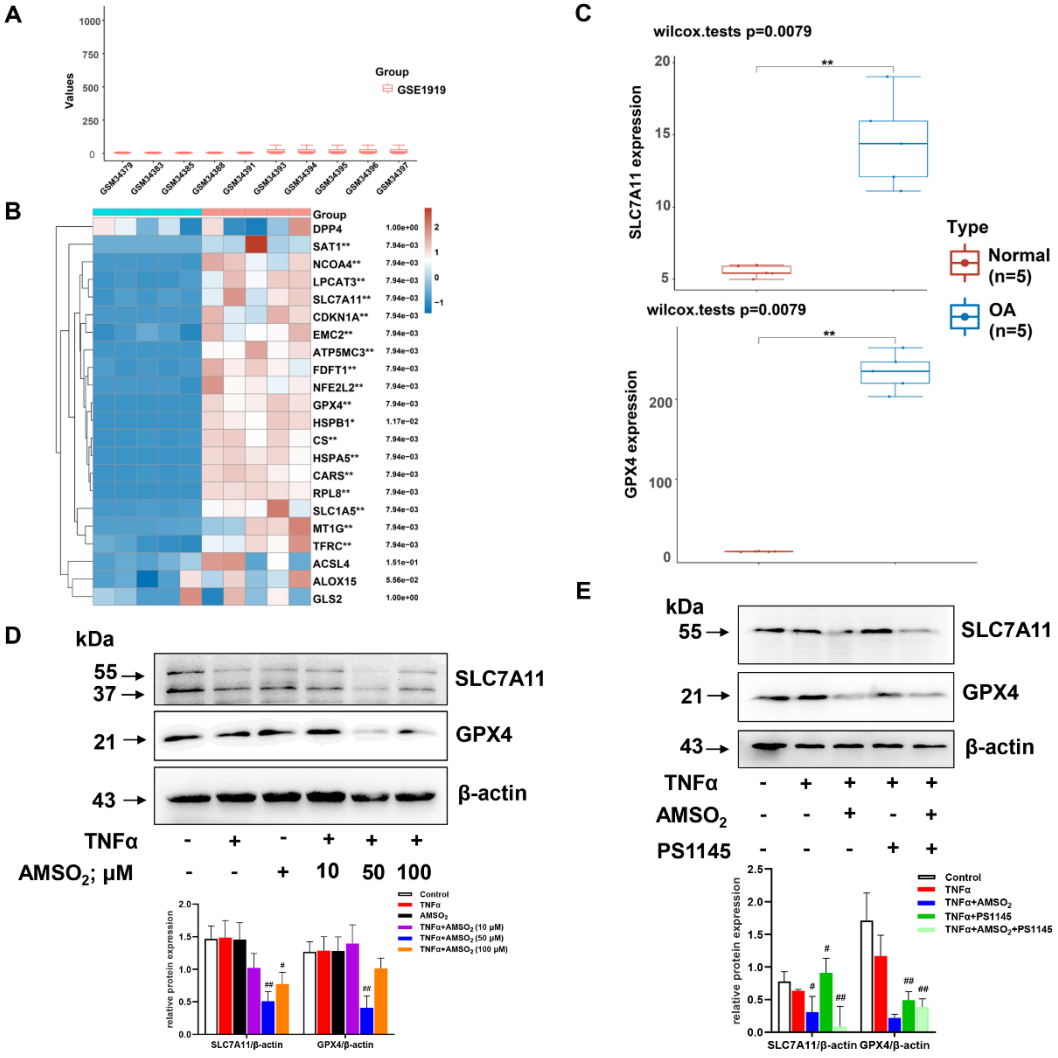

Figure 5. $AMSO_2$ regulated SLC7A11/GPX4 in TNFα-treated FLSs. (A) Boxplot of normalized data from the GEO dataset GSE1919. Rows represent samples, and columns represent gene expression values in the samples. (B) Heatmap of ferroptosis-related genes in synovial tissues (accession no. GSE1919, n = 5/group) between healthy individuals and patients with OA. Different colors represent the trend of gene expression in different samples. Statistical differences between the two groups were compared using the Wilcoxon test. *P < 0.05, **P < 0.01, ***P < 0.001. (C) The boxplots show the

expression distribution of Gpx4 and Slc7a11 in synovial tissues (accession no. GSE1919, n = 5/group) between healthy individuals and patients with OA. Statistical differences between the two groups were compared using the Wilcoxon test ($P < 0.01$). (D) The protein expression of SLC7A11 and GPX4 in $AMSO_2$ (50 μM)-treated FLSs was examined via western blotting. (E) The protein expression of SLC7A11 and GPX4 in the presence of PS1145 of $AMSO_2$ (50 μM)-treated FLSs. SLC7A11, cystine/glutamate transporter; GPX, glutathione peroxidase. Data were expressed as mean ± SD. All experiments were conducted in triplicate. *, $P < 0.05$ vs. control group; **, $P < 0.01$ vs. control group; #, $P < 0.05$ vs. TNFα group; ##, $P < 0. 01$ vs. TNFα group.**

3.6 $AMSO_2$ ameliorated OA development in the DMM-induced mice model

To evaluated the effect of $AMSO_2$ on subchondral bone remodeling in OA progression, the destabilization of the medial meniscus (DMM) was used to induce knee osteoarthritis (Fig. 6A). Following 35 days consecutive AMSO2 (100 mg/kg) administration, histological analyses were conducted. H&E, SF and TB staining were performed to evaluated the change of cartilage morphology and proteoglycan content (Fig. 6B-D). The OARSI score was significantly elevated ($P< 0.001$) in the DMM group, with substantial proteoglycan loss and surface erosion (Fig. 6E). However, the $AMSO_2$ treatment alleviated the morphology destruction, with restored surface smoothness and cartilage thickening after DMM, which showed a protective role in subchondral bone remodeling in OA progression.

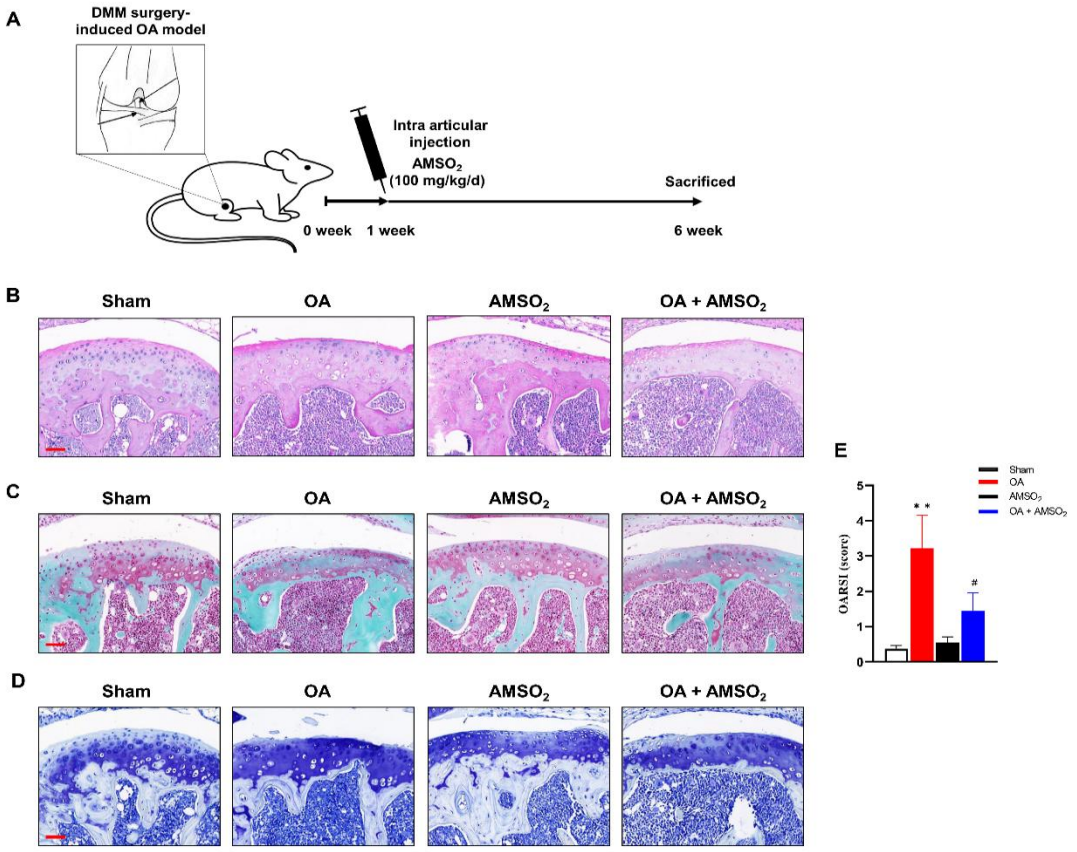

Figure 6. $AMSO_2$ ameliorates DMM-induced joint deterioration. (A) Schematic diagram of animal model establishment. Representative images of H&E (B), SO-FG (C) and TB (D) staining of knee joint sections from Sham, OA, $AMSO_2$, and $AMSO_2$-treated OA mice. Scale bar: 50 μm. (E) OARSI scores of the different groups. **, $P < 0.01$ vs. Sham group; #, $P < 0.05$ vs. OA group.

3. Discussion

Arthritis is characterized by articular cartilage damage, excessive ECM deposition, and synovial inflammation. In the present study, we demonstrated the effect of $AMSO_2$ on oxidative

and inflammatory responses in inflammatory FLSs. Arthritis is frequently characterized by synovial inflammation, and FLSs secrete a large number of chemical mediators that accelerate OA progression (R. Wang et al., 2021). Overactivated FLSs in the intima stimulate fibrogenesis via excessive ECM component deposition, leading to synovial hyperplasia. Furthermore, FLSs secrete cartilage-degrading enzymes, such as MMPs, thereby affecting the structure of the synovial membrane and leading to joint destruction. TNFα, one of the major proinflammatory cytokines in arthritis pathogenesis, activates overproliferation of synovial fibroblasts (Wu et al., 2022). In this study, TNFα-stimulated FLSs were used to mimic inflammatory circumstances in arthritis progression.

$AMSO_2$ is a major metabolite of garlic *in vivo*; it has been demonstrated to alleviate inflammation in acute lung injury (A. Li et al., 2018). In this study, the potent capacity of $AMSO_2$ was evaluated during the progression of OA; and the role of $AMSO_2$ in the regulation of oxidative stress and inflammation was further verified in TNFα-treated FLSs. $AMSO_2$ reduced the production of ROS and iNOS, and downregulated the expression of MMP-1, MMP-3, and MMP-13 in TNFα-stimulated FLSs. The effect of $AMSO_2$ have been mediated by the reduced production of chemokines, such as CCL2 and CCL5, leading to reduced monocyte infiltration in TNFα-treated FLSs.

Cartilage degradation is a well-recognized driving factor in the pathogenesis of arthritis. MMPs play a central role in the degradation of ECM collagens, which are overproduced from synovial cells, chondrocytes, and osteoblasts under inflammatory conditions. MMP-13 displays a preference for type II collagen (Davidson et al., 2006). MMP-1 and MMP-13 degrade type II collagen; they were originally referred to as collagenases 1 and 3, respectively; conversely, MMP-3 degrades both type II and IV collagen by disrupting collagen telopeptide cross-link. FLSs are activated by TNFα to secrete MMP-1, MMP-3, and MMP-13 (Chwastek, Kedziora, Borczyk, Korostynski, & Starowicz, 2022). So far, it is unclear how $AMSO_2$ affects MMP expression. The present study found that $AMSO_2$ significantly reduced TNFα-induced MMP expression, suggesting the ability of $AMSO_2$ to inhibit cartilage degradation. These results indicate the potential role of $AMSO_2$ in reducing oxidative stress and maintaining ECM balance in arthritis.

Upon exposure to TNFα, FLSs secrete proinflammatory cytokines, including IL-6, IL-8, and IL-1β, which initiate a signaling cascade to activate adaptive immune response (Liu, Feng, Wang, Zhao, & Li, 2017). TNFα further promotes ROS production, leading to oxidative stress. Oxidative stress, in turn, leads to increased ROS production in inflammatory joints, thereby promoting a positive feedback loop and long-term oxidative damage (Quinonez-Flores, Gonzalez-Chavez, Del Rio Najera, & Pacheco-Tena, 2016). Nitric oxide (NO) and iNOS have been shown to modulate ROS production in OA (Ahmad, Ansari, & Haqqi, 2020). In TNFα-treated FLSs, $AMSO_2$ reduced the expression of ROS and iNOS.

Proinflammatory cytokines and chemokines play crucial roles in various inflammatory diseases, including arthritis. CCL2 and IL-8 are potent recruiters of immune cells to the synovium and regulators of inflammatory response in RA (Yadav, Saini, & Arora, 2010). CCL2 binds to G protein-coupled receptors on monocytes to promote their activation and migration, whereas IL-8 attracts neutrophils to the synovium and has been considered the most important chemokine involved in arthritis. Our findings indicated that $AMSO_2$ significantly suppressed the expression of CCL2, IL-6, and IL-8 in inflammatory FLSs.

Inflammatory cytokines activated monocytes and macrophages and further increased immune cell recruitment to the synovium to promote cell damage. Monocyte-attracting cytokines, including CCL2 and TNFα, are implicated in OA and RA via mediation of monocyte migration (Mukai et al., 2021). Our study also demonstrated that $AMSO_2$ could inhibit THP-1 monocyte adhesion to inflammatory FLSs.

Recent studies have reported that promoting FLS apoptosis can prevent RA progression, which involves sirt1 translocation (Gu et al., 2016) and NF-κB activation (R. Wang et al., 2021). In synovial fibroblasts, NF-κB and mitogen-activated protein (MAP) kinase/activator protein 1 (AP-1) (c-Fos/c-Jun) play pivotal roles downstream of TNF. TNFα expression is induced by the activation of the NF-κB and MAPK pathways (Campbell et al., 2004). In this study,

we found that $AMSO_2$ ameliorated the increase in p65 activation and translocation induced by TNFα. PS1145 inhibits NF-κB translocation from the cytoplasm to the nucleus by impeding IκB kinase (IKK)-mediated IκB phosphorylation (Raskatov et al., 2012). The NF-κB pathway was blocked by PS1145 in $AMSO_2$-triggered FLSs. Thus, the effects of $AMSO_2$ may be mediated by the regulation of the NF-κB pathway in FLSs. These results indicate that $AMSO_2$ significantly inhibits the regulation of the NF-κB pathway, thereby suppressing the overactivation of FLSs under TNFα-induced inflammatory synoviocytes.

It has been demonstrated that NF-κB p65 can directly bind to SLC7A11 promoter, thus activating SLC7A11 transcription (Y. F. Wang et al., 2023). Based on the dataset GSE1919, SLC7A11 showed an obvious upregulation in OA synovium compared with normal. We supposed that the NF-κB p65/SLC7A11 signaling pathway is the major pathway in TNFα-stimulated FLSs with $AMSO_2$. Consistent with the changes in NF-κB p65, $AMSO_2$ decreased SLC7A11 and the downstream protein GPX4 expression in inflammatory FLSs.

Finally, *in vivo* study was conducted to access the effect of $AMSO_2$ by using surgical-induced subchondral bone destruction. The results showed that the DMM surgery induced cartilage degeneration, while $AMSO_2$ treatment mitigated the progression of OA.

4. Conclusions

Taken together, our findings suggest that $AMSO_2$ has a potential effect in OA protection, and the effect was mainly mediated through the inhibition of cartilage degradation caused by the inflammatory response and oxidative stress of FLSs. In this study, $AMSO_2$ suppressed the expression of SLC7A11 by targeting NF-κB p65; however, the underlying mechanism needs to be investigated in future studies. These results suggest that $AMSO_2$ may be used to treat inflammatory diseases with low toxicity.

Conflicting Interest

The authors declare no conflicts of interest.

Funding

This study was supported by the Natural Science Foundation of Shandong (grant number ZR2020QH073).

Authors Contributions

Zihao Dong: Conceptualization, Methodology, Software. **Yong Zhang:** Data curation, Writing-Original draft preparation. **Bin Li:** Visualization, Investigation. **Cuiling Gao:** Software, Validation. **Guodong Wang:** Methodology, Software. **Guang Yang:** Supervision, Writing-Reviewing and Editing.

Data Statement

The original contributions presented in this study are included in the article/supplementary material. Further inquiries can be directed to the corresponding author(s). Microarray and RNA-seq data generated in this study have been deposited in the Gene Expression Omnibus under accession code GSE1919.

References

1. Ahmad, N., Ansari, M. Y., & Haqqi, T. M. (2020). Role of iNOS in osteoarthritis: Pathological and therapeutic aspects. *J Cell Physiol, 235*(10), 6366-6376. doi:10.1002/jcp.29607
2. Bao, J., Yan, W., Xu, K., Chen, M., Chen, Z., Ran, J., . . . Wu, L. (2020). Oleanolic Acid Decreases IL-1beta-Induced Activation of Fibroblast-Like Synoviocytes via the SIRT3-NF-kappaB Axis in Osteoarthritis. *Oxid Med Cell Longev, 2020*, 7517219. doi:10.1155/2020/7517219
3. Bolduc, J. A., Collins, J. A., & Loeser, R. F. (2019). Reactive oxygen species, aging and articular cartilage homeostasis. *Free Radic Biol Med, 132*, 73-82. doi:10.1016/j.freeradbiomed.2018.08.038
4. Cai, D., Yan, H., Liu, J., Chen, S., Jiang, L., Wang, X., & Qin, J. (2021). Ergosterol limits osteoarthritis development and progression through activation of Nrf2 signaling. *Exp Ther Med, 21*(3), 194. doi:10.3892/etm.2021.9627
5. Campbell, J., Ciesielski, C. J., Hunt, A. E., Horwood, N. J., Beech, J. T., Hayes, L. A., . . . Foxwell, B. M. (2004). A novel mechanism for TNF-alpha regulation by p38 MAPK: involvement of NF-kappa B with implications for therapy in rheumatoid arthritis. *J Immunol, 173*(11), 6928-6937. doi:10.4049/jimmunol.173.11.6928
6. Chen, W. C., Lin, C. Y., Kuo, S. J., Liu, S. C., Lu, Y. C., Chen, Y. L., . . . Tang, C. H. (2020). Resistin Enhances VCAM-1 Expression and Monocyte Adhesion in Human Osteoarthritis

Synovial Fibroblasts by Inhibiting MiR-381 E xpression through the PKC, p38, and JNK Sig naling Pathways. *Cells, 9*(6). doi:10.3390/cells 9061369
7. Chen, W. C., Wang, S. W., Lin, C. Y., Tsai, C. H., Fong, Y. C., Lin, T. Y., . . . Tang, C. H. (20 19). Resistin Enhances Monocyte Chemoattra ctant Protein-1 Production in Human Synovial Fibroblasts and Facilitates Monocyte Migratio n. *Cell Physiol Biochem, 52*(3), 408-420. doi:1 0.33594/000000029
8. Chwastek, J., Kedziora, M., Borczyk, M., Kor ostynski, M., & Starowicz, K. (2022). Inflam mation-Driven Secretion Potential Is Upregula ted in Osteoarthritic Fibroblast-Like Synovioc ytes. *Int J Mol Sci, 23*(19). doi:10.3390/ijms23 1911817
9. Dasuri, K., Antonovici, M., Chen, K., Wong, K., Standing, K., Ens, W., . . . Wilkins, J. A. (2 004). The synovial proteome: analysis of fibro blast-like synoviocytes. *Arthritis Res Ther, 6* (2), R161-168. doi:10.1186/ar1153
10. Davidson, R. K., Waters, J. G., Kevorkian, L., Darrah, C., Cooper, A., Donell, S. T., & Clark, I. M. (2006). Expression profiling of metallopr oteinases and their inhibitors in synovium and cartilage. *Arthritis Res Ther, 8*(4), R124. doi:1 0.1186/ar2013
11. Gu, X., Gu, B., Lv, X., Yu, Z., Wang, R., Zho u, X., . . . Jin, J. (2016). 1, 25-dihydroxy-vitam in D3 with tumor necrosis factor-alpha protect s against rheumatoid arthritis by promoting p5 3 acetylation-mediated apoptosis via Sirt1 in s ynoviocytes. *Cell Death Dis, 7*(10), e2423. do i:10.1038/cddis.2016.300
12. Haraden, C. A., Huebner, J. L., Hsueh, M. F., Li, Y. J., & Kraus, V. B. (2019). Synovial fluid biomarkers associated with osteoarthritis sever ity reflect macrophage and neutrophil related i nflammation. *Arthritis Res Ther, 21*(1), 146. d oi:10.1186/s13075-019-1923-x
13. Ishii, S., Isozaki, T., Furuya, H., Takeuchi, H., Tsubokura, Y., Inagaki, K., & Kasama, T. (201 8). ADAM-17 is expressed on rheumatoid arth ritis fibroblast-like synoviocytes and regulates proinflammatory mediator expression and mo nocyte adhesion. *Arthritis Res Ther, 20*(1), 15 9. doi:10.1186/s13075-018-1657-1
14. Katz, J. N., Arant, K. R., & Loeser, R. F. (202 1). Diagnosis and Treatment of Hip and Knee Osteoarthritis: A Review. *JAMA, 325*(6), 568-578. doi:10.1001/jama.2020.22171
15. Li, A., Liu, Y., Zhu, X., Sun, X., Feng, X., Li, D., . . . Zhao, Z. (2018). Methylallyl sulfone at tenuates inflammation, oxidative stress and lu ng injury induced by cigarette smoke extract i n mice and RAW264.7 cells. *Int Immunophar macol, 59*, 369-374. doi:10.1016/j.intimp.201 8.04.028
16. Li, S., He, Y., Chen, K., Sun, J., Zhang, L., He, Y., . . . Li, Q. (2021). RSL3 Drives Ferroptosis through NF-kappaB Pathway Activation and GPX4 Depletion in Glioblastoma. *Oxid Med C ell Longev, 2021*, 2915019. doi:10.1155/2021/ 2915019
17. Liu, N., Feng, X., Wang, W., Zhao, X., & Li, X. (2017). Paeonol protects against TNF-alpha -induced proliferation and cytokine release of rheumatoid arthritis fibroblast-like synoviocyt es by upregulating FOXO3 through inhibition of miR-155 expression. *Inflamm Res, 66*(7), 6 03-610. doi:10.1007/s00011-017-1041-7
18. Liu, S., Cao, C., Zhang, Y., Liu, G., Ren, W., Y e, Y., & Sun, T. (2019). PI3K/Akt inhibitor par tly decreases TNF-alpha-induced activation of fibroblast-like synoviocytes in osteoarthritis. *J Orthop Surg Res, 14*(1), 425. doi:10.1186/s130 18-019-1394-4
19. Liu, Y., Li, A., Jiang, X., Zhu, X., Feng, X., Su n, X., & Zhao, Z. (2019). Metabolism and pha rmacokinetics studies of allyl methyl disulfide in rats. *Xenobiotica, 49*(1), 90-97. doi:10.1080 /00498254.2017.1419309
20. Mateen, S., Zafar, A., Moin, S., Khan, A. Q., & Zubair, S. (2016). Understanding the role of cytokines in the pathogenesis of rheumatoid ar thritis. *Clin Chim Acta, 455*, 161-171. doi:10.1 016/j.cca.2016.02.010
21. Mathiessen, A., & Conaghan, P. G. (2017). Sy novitis in osteoarthritis: current understanding with therapeutic implications. *Arthritis Res Th er, 19*(1), 18. doi:10.1186/s13075-017-1229-9
22. Mukai, M., Uchida, K., Okubo, T., Takano, S., Matsumoto, T., Satoh, M., . . . Takaso, M. (202 1). Regulation of Tumor Necrosis Factor-alpha by Peptide Lv in Bone Marrow Macrophages and Synovium. *Front Med (Lausanne), 8*, 702 126. doi:10.3389/fmed.2021.702126
23. Nygaard, G., & Firestein, G. S. (2020). Restori ng synovial homeostasis in rheumatoid arthriti s by targeting fibroblast-like synoviocytes. *Nat Rev Rheumatol, 16*(6), 316-333. doi:10.1038/s 41584-020-0413-5
24. Ostojic, M., Zevrnja, A., Vukojevic, K., & Solj

ic, V. (2021). Immunofluorescence Analysis of NF-kB and iNOS Expression in Different Cell Populations during Early and Advanced Knee Osteoarthritis. *Int J Mol Sci, 22*(12). doi:10.3390/ijms22126461

25. Perez-Garcia, S., Carrion, M., Villanueva-Romero, R., Hermida-Gomez, T., Fernandez-Moreno, M., Mellado, M., . . . Gomariz, R. P. (2019). Wnt and RUNX2 mediate cartilage breakdown by osteoarthritis synovial fibroblast-derived ADAMTS-7 and -12. *J Cell Mol Med, 23*(6), 3974-3983. doi:10.1111/jcmm.14283
26. Qin, Y., Cai, M. L., Jin, H. Z., Huang, W., Zhu, C., Bozec, A., . . . Chen, Z. (2022). Age-associated B cells contribute to the pathogenesis of rheumatoid arthritis by inducing activation of fibroblast-like synoviocytes via TNF-alpha-mediated ERK1/2 and JAK-STAT1 pathways. *Ann Rheum Dis, 81*(11), 1504-1514. doi:10.1136/ard-2022-222605
27. Quinonez-Flores, C. M., Gonzalez-Chavez, S. A., Del Rio Najera, D., & Pacheco-Tena, C. (2016). Oxidative Stress Relevance in the Pathogenesis of the Rheumatoid Arthritis: A Systematic Review. *Biomed Res Int, 2016*, 6097417. doi:10.1155/2016/6097417
28. Raghu, H., Lepus, C. M., Wang, Q., Wong, H. H., Lingampalli, N., Oliviero, F., . . . Robinson, W. H. (2017). CCL2/CCR2, but not CCL5/CCR5, mediates monocyte recruitment, inflammation and cartilage destruction in osteoarthritis. *Ann Rheum Dis, 76*(5), 914-922. doi:10.1136/annrheumdis-2016-210426
29. Raskatov, J. A., Meier, J. L., Puckett, J. W., Yang, F., Ramakrishnan, P., & Dervan, P. B. (2012). Modulation of NF-kappaB-dependent gene transcription using programmable DNA minor groove binders. *Proc Natl Acad Sci U S A, 109*(4), 1023-1028. doi:10.1073/pnas.1118506109
30. Wang, R., Li, J., Xu, X., Xu, J., Jiang, H., Lv, Z., . . . Shi, D. (2021). Andrographolide attenuates synovial inflammation of osteoarthritis by interacting with tumor necrosis factor receptor 2 trafficking in a rat model. *J Orthop Translat, 29*, 89-99. doi:10.1016/j.jot.2021.05.001
31. Wang, Y. F., Feng, J. Y., Zhao, L. N., Zhao, M., Wei, X. F., Geng, Y., . . . Zhang, X. D. (2023). Aspirin triggers ferroptosis in hepatocellular carcinoma cells through restricting NF-kappaB p65-activated SLC7A11 transcription. *Acta Pharmacol Sin, 44*(8), 1712-1724. doi:10.1038/s41401-023-01062-1
32. Wu, J., Feng, Z., Chen, L., Li, Y., Bian, H., Geng, J., . . . Zhu, P. (2022). TNF antagonist sensitizes synovial fibroblasts to ferroptotic cell death in collagen-induced arthritis mouse models. *Nat Commun, 13*(1), 676. doi:10.1038/s41467-021-27948-4
33. Xie, C., & Chen, Q. (2019). Adipokines: New Therapeutic Target for Osteoarthritis? *Curr Rheumatol Rep, 21*(12), 71. doi:10.1007/s11926-019-0868-z
34. Yadav, A., Saini, V., & Arora, S. (2010). MCP-1: chemoattractant with a role beyond immunity: a review. *Clin Chim Acta, 411*(21-22), 1570-1579. doi:10.1016/j.cca.2010.07.006
35. Yang, G., Sun, S., Wang, J., Li, W., Wang, X., Yuan, L., & Li, S. (2020). S-Allylmercaptocysteine Targets Nrf2 in Osteoarthritis Treatment Through NOX4/NF-kappaB Pathway. *Drug Des Devel Ther, 14*, 4533-4546. doi:10.2147/DDDT.S258973
36. Yang, M., Dong, Z., Jiang, X., Zhao, Z., Zhang, J., Cao, X., & Zhang, D. (2018). Determination of S-Allylmercaptocysteine in Rat Plasma by LC-MS/MS and its Application to a Pharmacokinetics Study. *J Chromatogr Sci, 56*(5), 396-402. doi:10.1093/chromsci/bmy001